Structural and Optical Properties of RF-Sputtered CdTe Thin Films Grown on CdS:O/CdS Bilayers

N. K. Das*‡, S. F. U. Farhad**, J. Chakaraborty*, A. K. S. Gupta*, M. Dey*, M. Al- Mamun***, M. A. Matin*, N. Amin****

*Department of EEE, Chittagong University of Engineering and Technology, Chittagong-4349, Bangladesh

** Industrial Physics Division, Bangladesh Council of Scientific and Industrial Research, Dhaka-1205, Bangladesh

*** Materials Science Division, Atomic Energy Center, Bangladesh Atomic Energy Commission, Dhaka-1205, Bangladesh

**** Institute of Sustainable Energy, UniversitiTenagaNasional, 43000 Kajang, Selangor, Malaysia

(nipudas@cuet.ac.bd, sf1878@my.bristol.ac.uk, joychakr@cuet.ac.bd, ashoke.cuet.eee@gmail.com, mrinmoy@cuet.ac.bd, mamunfh@yahoo.com, imamatin@yahoo.com, nowshad@uniten.edu.my)

‡Corresponding Author; N. K. Das, Department of EEE, Chittagong University of Engineering and Technology, Chittagong-4349, Bangladesh, Tel: +8801732051996, nipudas@cuet.ac.bd

Received: 20.01.2020 Accepted:25.02.2020

Abstract- In this work, we report the structural and optical properties of CdTe thin films on Oxygenated Cadmium Sulfide (CdS:O)/Cadmium Sulfide (CdS) bilayers using RF magnetron sputtering for different substrate temperatures (150, 200, 250, 300 and 350 °C) in Argon ambient. The XRD spectra reveal the polycrystalline nature of all the CdTe thin films with preferential cubic orientation along (111) directions. Raman Spectra show the dominant peak at 163.5 cm^{-1} and its overtone at 328.7 cm^{-1} which corresponds to the longitudinal optical (LO) phonon of CdTe. The SEM microscopy exhibits the uniform growth of CdTe films onto the entire glass substrate. Improved spectral response is observed for CdS:O layer and CdS:O/CdS bilayer in comparison with the CdS layer. The optical transmission of the CdTe films begins at the edge of 800 nm wavelength and shows interference fringe in the transmission spectra. The thickness of the deposited films and the optical constants are calculated from the fringe pattern. The thicknesses of the CdTe films are found to be increasing from 2.34 μm to 2.82 μm with the increasing substrate temperature i.e. from 150 to 250°C. Thereafter, the CdTe film thickness decreases to 2.24 μm while the temperature increases further up to 350°C. The optical bandgap of the deposited CdTe films follows an increasing trend of 1.48 eV to 1.54 eV with the increase of substrate temperature 150 to 250°C after that the bandgap decreases to 1.51 eV for 350°C. Hence the obtained structural and optical properties suggest that the deposited CdTe films can be used as a suitable absorber layer for the thin film-based solar cells.

Keywords CdTe; thin film; RF sputtering; substrate temperature; optical constants; crystallite size.

1. Introduction

CdTe is a leading absorber material for manufacturing the least cost and efficient thin-film solar cells for terrestrial utilization [1-2]. At present, the photovoltaic conversion efficiency of a heterojunction CdTe solar cell reaches 22.1 % and 18.6 % respectively for laboratory-scale cell and module respectively [3-4]. It is expected that in the near future, the cell efficiency of 24 ~ 25 % can be achieved by improving the material properties of the CdTe absorber layer [5]. CdTe material has a direct bandgap of (1.44 -1.56) eV and has high absorption coefficient $\alpha \approx 2\times10^4$ cm^{-1} at $\lambda \approx 820$ nm [6-8] which in turn allows it to convert 92 % of the useful sunlight into electricity by using only 1 μm thick CdTe material. Moreover, CdTe material showed amphoteric behavior as it is possible to dope both n-type and p-type by intrinsically and extrinsically. The acceptor density of intrinsically deposited CdTe thin-film is near about 10^{13} ~ 10^{14} cm^{-3} mostly due to the presence of native defects (Cadmium vacancies V_{Cd}), chemical impurities (Na, Cu, Ag) and

complexes $(Cl_{Te}^{+} - V_{Cd}^{2-})^{-}$ [6, 9-10]. The low acceptor densities of CdTe material create strong challenges in the further improvement of the CdTe cell efficiency mostly due to the open-circuit voltage *Voc* (*Voc*< 1 V) limitation relative to its potential [11-13]. On the other hand, the inherent self-compensation property of the CdTe material limits the efficient p-type doping (N, P, As, Sb) of the order of $10^{15}cm^{-3}$ [5, 14-15]. Thus, further improvement of the CdTe solar cell highly depends on the quality of CdTe absorber layer deposition, since the physical and optical-electrical properties of the CdTe absorber layer is highly dependent on the deposition process and deposition methods. There are various physical and chemical deposition method available for synthesizing CdTe thin films such as chemical bath deposition (CBD) [16], close-spaced sublimation (CSS) [17], thermal evaporation [18-19], sputtering [20], spray pyrolysis [21], physical vapour deposition (PVD) [22], electrode deposition [23-24], metal-organic chemical vapour deposition (MOCVD) [25], molecular beam epitaxy (MBE) [26] and pulse laser ablation [27]. Usually, the thickness of the deposited CdTe thin films in the range of 2 to 10 μm and the substrate temperatures are varies from 80 to 650 °C depending upon the deposition methods.

Generally, RF magnetron sputtering is a high vacuum and medium temperature thin film deposition technique that permits a very dense, homogenous and uniform coverage, controllable film thickness and provides better adhesion with the glass substrate [28]. Several recent studies reported that the properties of the as-deposited CdTe thin films which were grown onto the glass substrate with different process parameters such as substrate temperature, RF power and process pressure during deposition [29-33]. As it is well known that the performance of the CdTe solar cell hinders by strong parasitic absorption of the CdS window layer [33-36]. As a consequence, in this work, we used a bilayer of CdS:O/CdS to improve the optical spectral response of the window layer and observed its effect on the structural and optical properties of CdTe films as the function of the substrate temperature.

2. Experimental Details

2.1. *Growth of CdS:O/CdS/CdTe thin-films*

In this work commercially available soda-lime glass (SLG) substrates (25mm×75mm×1mm) were used for the deposition of the CdS:O/CdS/CdTe stack layer using RF magnetron sputtering. The SLG substrates were cleaned by a standard cleaning procedure as described in [37] and then dried by using nitrogen gas. Subsequently, the clean substrates were dried on a hot plate at 150°C for removing dirt and moisture. In Fig. 1, the SLG substrate cleaning process is shown. The clean substrate then was mounted into the substrate holder and the distance between source and substrate was maintained to 7 cm. Analytical grade 99.99 % pure CdS and CdTe target material were fitted to RF sputtering gun-1 and gun-2 respectively. RF sputtering chamber was pump down to 5.21×10^{-5} Torr by turbomolecular and backing pump before deposition. Thereafter, 16 sccm of Ar gas was flown into the vacuum chamber through mass flow controller (MFC) and the process pressure was maintained to 3.06 mTorr. The CdS layer was deposited at room temperature (RT) 25 °C onto the SLG substrate for 30 W RF power. Thereafter, 16 sccm of Ar gas and 0.25 sccm of O_2 were flown into the vacuum chamber through mass flow controller (MFC) and the process pressure was maintained to 3.21 mTorr. Then, the CdS:O layer was deposited by reactive sputtering at RT for RF power 30 W.

Standard chemical solution (Methanol, Acetone and DI water) and ultrasonic bath

Drying of SLG substrate through nitrogen gas and on Hot plate.

Fig. 1. Ultrasonically cleaning and drying of SLG glass substrate

The CdS:O/CdS stack layer was deposited by the same recipe but the CdS layer was deposited over the CdS:O layer at 250 °C substrate temperature in pure Ar ambient. After that, CdTe thin films were deposited for the substrate temperature 150, 200, 250, 300 and 350 °C respectively and the deposited films are shown in Fig. 2. The detail deposition process parameter is presented in Table 1.

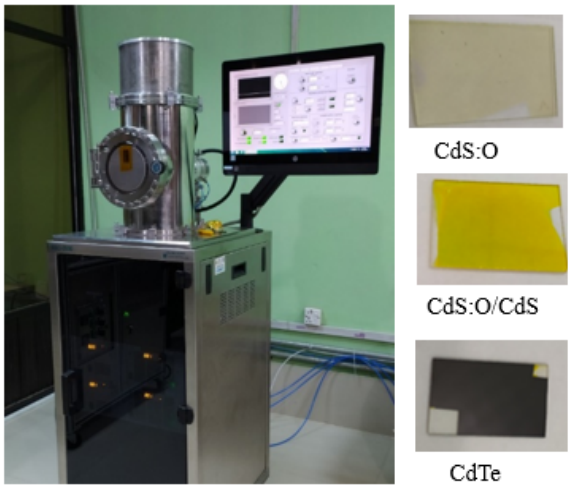

Deposition of CdS:O/CdS/CdTe thin-films by RF Sputtering.

Fig. 2. Photograph of two gun RF sputtering coater with CdS:O, CdS:O/CdS and CdS:O/CdS/CdTe layers.

Table 1. Deposition parameters of CdS, CdS:O, CdTe thin films.

Process parameters	CdS thin films	CdS:O/CdS/ CdTe layer stack		
		1st layer CdS:O	2nd layer CdS	3rd layer CdTe
RF Power	30 W	30 W	30 W	50 W
Deposition Pressure	3.06 mTorr	3.21 mTorr	3.21 mTorr	3.80 mTorr
Ar gas flow	16 sccm	16 sccm	16 sccm	20 sccm
O_2/(Ar+ O_2) ratio	0 %	1.5 %	0 %	0 %
Substrate Temperature	25 °C	25 °C	250 °C	150 °C ~ 350 °C
Thickness of CdS films	~ 350 nm	~ 120 nm	~ 150 nm	2.5 ~4 µm
Deposition time	60 minutes	30 minutes	30 minutes	180 minutes
Source to substrate distance	7 cm	7 cm	7 cm	7 cm

2.2. *Characterization of as-grown films*

The optical properties of CdS, CdS:O, CdS:O/CdS and CdS:O/CdS/CdTe deposited films were investigated by SHIMADZU UV-2600, UV-Vis NIR spectrophotometer for optical wavelength 220 nm to 1400 nm. The structural properties of all the deposited films were carried out by Panalytical XRD whose Cu-Kα X-ray radiation λ = 0.15408 nm. Further, the impurity and crystalline defects of all the deposited CdS:O/CdS/CdTe stack layers were investigated by Raman spectroscopy. Besides, the surface morphology and compositional properties of the as-grown CdTe thin film deposited at 250 °C was inspected with the field emission scanning electron microscope (FESEM).

3. Results and discussion

3.1. *Structural Properties*

The structural properties of as-grown CdS thin-film, CdS:O thin-film, CdS:O/CdS bilayer and the CdS:O/CdS/CdTe stack layer were investigated by XRD. The XRD patterns of the aforementioned as-deposited films and stack layers are shown in Fig. 3. It is observed from the XRD spectra that the RT deposited CdS films show polycrystalline nature with the preferential orientation of hexagonal wurtzite peak along the (002) plane. In contrast, the CdS:O films deposited in the presence of 1.5% O_2/Ar ratio at RT show no identifiable intense peak which indicates no crystallization at this condition. Again, the CdS:O/CdS stack layer deposited at 250 °C shows preferential crystalline orientation at (002) plane. The diffraction pattern of CdTe thin films deposited at 150 °C also shows polycrystalline nature and the XRD peaks are found at 2θ ≈ 23.66°, 39.1°, 46.51°, 57.4°, 72.22° correspondingly for (111), (220), (311), (400) and (422) plane. Whereas the prominent peak in the (111) plane denotes the stable zinc-blend crystal orientation of CdTe and this is a preferred orientation for the fabrication of CdTe solar cell. A comparative XRD pattern of (111) peak location for different substrate temperatures has shown in Fig. 4. The crystal lattice constant of the cubic phase of CdTe and hexagonal wurtzite phase of the CdS thin films are calculated by the Bragg's law [30]:

$$d_{hkl} = \frac{\lambda}{2} \times \cos ec(\theta) \quad (1)$$

$$a_c = d_{hkl}\left(h^2 + k^2 + l^2\right)^{\frac{1}{2}} \quad (2)$$

Where d is the inter planar spacing in the atomic lattice, λ is the wavelength of the X-ray radiation and θ refers to the angle between incident X-ray and scattering crystallographic planes. The lattice parameter of the hexagonal unit cell is closely related to cubic lattice parameters of the same material by Vegard's law.

$$a_{hex} = (1/2)^{\frac{1}{2}} a_c \quad (3a)$$

$$c_{hex} = (4/3)^{\frac{1}{2}} a_c \quad (3b)$$

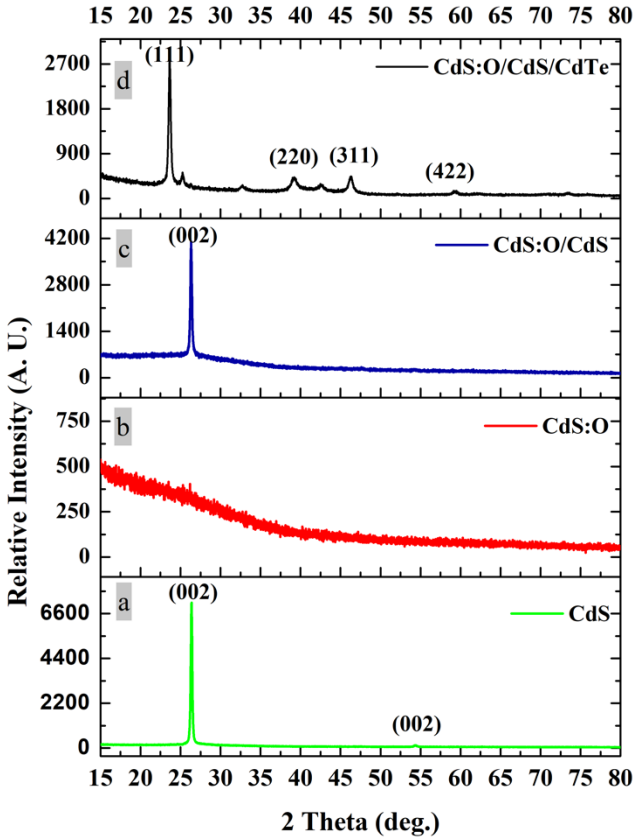

Fig. 3. XRD pattern of the deposited films (a) CdS at RT (b) CdS:O at RT (c) CdS:O (RT)/CdS (250°C) and (d) CdS:O (RT)/CdS/CdTe at 150°C.

The crystallite size D, micro-strain ε, and dislocation density δ of the aforementioned CdS, CdS:O/CdS bilayer and CdS:O thin films. This might be due to compressive stress induced in the crystal lattice as it is deposited over nanocrystalline CdS:O films. The estimated values of the structural properties are consistent with the related work [38]. Meanwhile, it is found that the crystallinity and the crystallite size of the CdTe films increased with the increase of substrate temperature up to 300 °C and then it is decreased for 350° C. The lattice constant of the as-deposited CdTe is higher than its ideal values (a= 6.480) [8] for the CdTe films deposited at 150 and 200 °C which is the indication of induced compressive stress in these deposited films. Meanwhile, the estimated lattice constant was found closer to its ideal values for the substrate temperature 250 and 300 °C and then it again increased as we increase the substrate temperature to 350 °C.

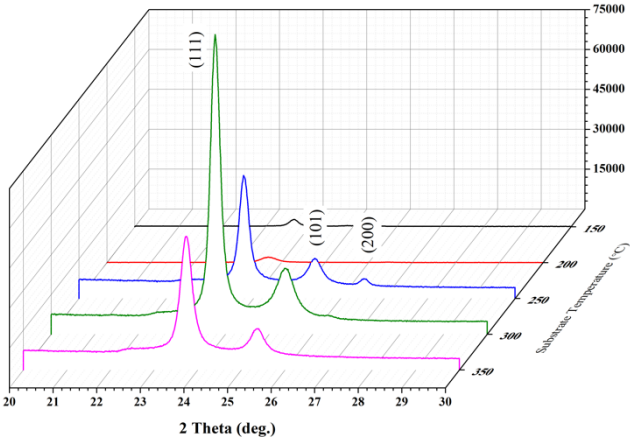

Fig. 4. Comparative XRD pattern of CdTe thin films for different substrate temperature showing (111) the peak intensity for the tri-layer structures CdS:O/CdS/CdTe. The process parameters of each layer are shown in Table 1.

CdTe thin films are calculated using Scherer formula and Williamson and Smallman's relation accordingly;

$$D_{hkl} = \frac{K\lambda}{\beta_{2\theta}\cos\theta} \quad (4)$$

$$\varepsilon = \frac{\beta_{2\theta}}{4\tan\theta} \quad (5)$$

$$\delta = \frac{n}{D^2} \quad (6)$$

Where K is the Scherer's constant (K ≈ 0.89), $\beta_{2\theta}$ is full-width half maxima and n is a factor and it is considered as unity for minimum dislocation densities. The estimated values of the lattice constant, average crystallite size, micro-strain, and the dislocation densities are presented in Table 2.

Table 2. Structural Properties of the deposited thin films.

Samples	Substrate temperature	d(hkl) (nm)	Lattice constant a (Å)	Crystallite size (nm)	Micro strain ε ($\times 10^{-3}$)
CdS	25 °C	3.37	4.772	35.15	4.31
CdS:O/CdS	25 °C/ 250 °C	3.38	4.781	30.76	4.94
CdTe-01	150 C	3.76	6.504	23.86	7.08
CdTe-02	200 °C	3.75	6.497	26.85	6.28
CdTe-03	250 °C	3.74	6.477	32.83	5.12
CdTe-04	300 °C	3.74	6.483	33.28	5.06
CdTe-05	350 °C	3.75	6.490	27.81	6.07

As can be seen from this Table 2, the crystallite size of the deposited CdS thin films at RT for one hour duration has a larger crystallite size than the CdS film deposited onto

3.2. Optical properties

The optical transmission spectra of all the deposited CdTe thin films are grown onto CdS:O/CdS bilayer for different substrate temperatures as shown in Fig. 5. As seen in Fig. 5 the optical transmission is shifted to the blue region (330 nm) as we incorporated 1.5 % oxygen into the sputtering chamber in comparison with the CdS films that were deposited in pure Ar ambient. Meanwhile, the optical transmission edges slightly shifted to 470 nm as we bilayer the CdS:O layer with the CdS:O/CdS layer. Furthermore, the transmission edges of all the deposited CdTe films atop of CdS:O/CdS bilayer begins near 800 nm of photon wavelength which confirms the complete absorption of the visible wavelength of the sunlight spectrum.

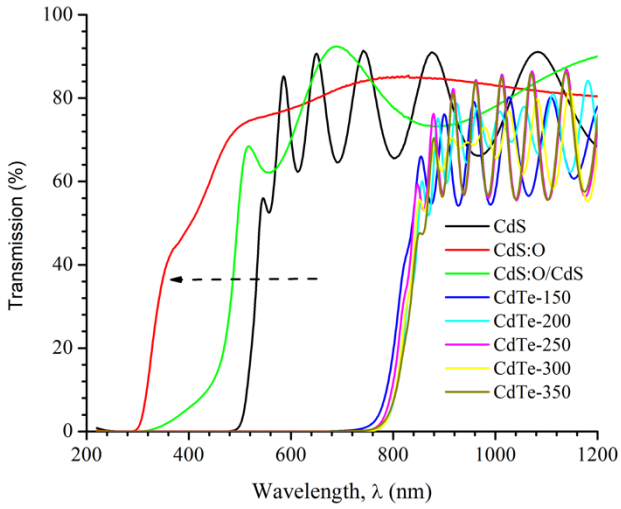

Fig.5. Transmission spectra of all the deposited thin films.

These phenomena suggesting that all the deposited CdTe films are suitable to use as an absorber layer for solar cells. Moreover, all the CdTe films showed optical transmission over 65 % after the tranmission edge of 820 nm wavelength and interference fringe which is the indication of good crystallinity and smooth surface morphology of the deposited films. From the fringe pattern, the optical constants (refractive index n, absorption coefficient α and extinction coefficient k) and the thickness of the deposited films are calculated by using envelope function as in [39]. The

envelope function is shown in Fig. 6 for the CdTe films deposited at 250 °C.

The refractive index n is calculated for all the deposited films by the following expression:

$$n = [N + (N^2 - n_0^2 n_1^2)^{1/2}]^{1/2} \quad (7)$$

$$N = \frac{n_0^2 + n_1^2}{2} + 2n_0 n_1 \frac{T_{max} - T_{min}}{T_{max} T_{min}} \quad (8)$$

Where n_0, n_1 is the refractive index of air and the glass substrate and T_{max}, T_{min} is the corresponding maxima and minima at the same wavelength of the envelope function. The estimated values of refractive index is found in the range of 2.4 to 2.5, which is consistent with the other reported results [40-41].

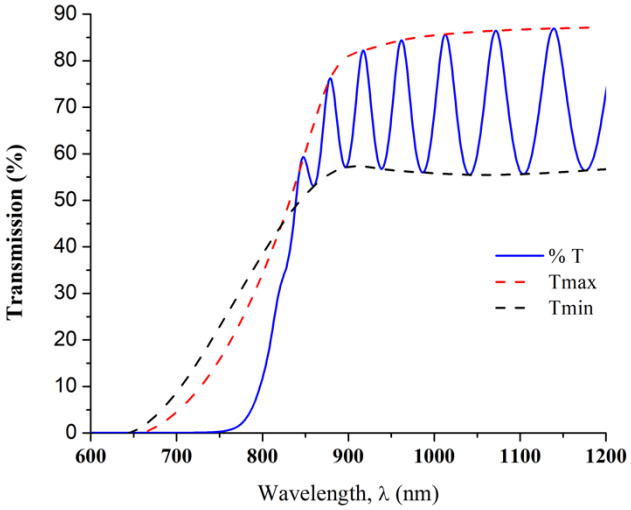

Fig. 6. Transmission spectrum with envelope curve for the CdTe thin film deposited at 250 °C.

The thickness t for all the deposited films were calculated from two consecutive maxima or minima by Eq. (9) [39].

$$t = \frac{M\lambda_1\lambda_2}{2\{n(\lambda_1)\lambda_2 - n(\lambda_2)\lambda_1} \quad (9)$$

Where M is the number of oscillation between the two extrema occurring for λ_1 and λ_2 and $n(\lambda_1)$ and $n(\lambda_2)$ being the corresponding refractive indices of the deposited film. The calculated thickness of the deposited CdTe films is shown in Table 3.

Table 3. Calculated thickness of the deposited thin films

Sample ID	Substrate Temp. (°C)	Thickness (μm)	Deposition Rate (Å /S)
CdTe-01	150	2.34	2.17
CdTe-02	200	2.51	2.32
CdTe-03	250	2.82	2.61
CdTe-04	300	2.61	2.42
CdTe-05	350	2.24	2.07

As observed in Table 3, the thickness of deposited CdTe films increases as the substrate temperature increases from 150 °C and reaches a maximum of 2.82 μm at 250 °C and then the film thickness slightly decreases to 2.61 μm for substrate temperature 300 °C. Finally, abrupt decrement of CdTe film thickness to 2.24 μm is observed decreases abruptly to 2.24 μm as the temperature increase further up to 350 °C. The abrupt reduction of film thickness might be due to the lower condensation rate of the emitted Cd and Te vapour on the glass substrate at elevated substrate temperature > 300 °C. Hence, the optimum substrate temperature for growing CdTe thin film on the glass substrate is between 250 to 300 °C and this value is consistent with the other related reports [20, 42-43].

As we know in the fundamental absorption region, the values of absorption coefficient α are calculated from the transmission spectra by the following expression:

$$\alpha = \frac{1}{t} \ln\left(\frac{1}{T}\right) \quad (10)$$

Where T and t are the transmittance and thickness of the deposited CdTe thin film respectively. Moreover, it is well known that the velocity of propagation of an electromagnetic wave through a solid film is given by the frequency-dependent complex refractive index $\eta = n - ik$ where the real part, n is related to the velocity and k, is the extinction coefficient which is related to the damping of the oscillation amplitude of the incident electric field. The velocity of propagation of a plane wave of frequency (f) which propagates through a thin solid film is related to velocity (v) in a direction defined by (x), the electric field (E) is described by the following time-dependent (t) progressive wave equation.

$$E = E_0 \exp\{i2\pi f[t - (x/v)]\} \quad (11)$$

Meanwhile the velocity of propagation of complex refractive index η is related to the speed of light in a vacuum, c, by $v = c / \eta$, then:

$$\frac{1}{v} = \frac{n}{c} - \frac{ik}{c} \quad (12)$$

Therefore, substituting $1/v$ into the equation above produces:

$$E = E_0 \exp(i2\pi ft) \exp\left(\frac{-i2\pi xnf}{c}\right) \exp\left(\frac{-2\pi fkx}{c}\right) \quad (13)$$

Where the last term, $-2\pi fkx/c$ is a measure of the damping factor, or extinction coefficient (k) of the solid films. As the intensity (P) of an incident wave through a solid is the conductivity (σ) of the solid multiplied by the square of the electric field vector ($P=\sigma E^2$), then using the damping factor term, the fraction of the incident power that has propagated from position (o) to a distance (x) through the material with conductivity (σ) is given by:

$$\frac{P(x)}{P(0)} = \frac{\sigma E^2(x)}{\sigma E^2(0)} = \exp\left(\frac{-4\pi fkx}{c}\right) \quad (14)$$

The Eq. (14) signifies the intensity of the incident radiation which is attenuated by the solid to $1/e$ of its initial value at a distance from the surface boundary defined by $c/4\pi fk$ and the

absorption coefficient (α) can be expressed in terms of the extinction coefficient (k) as:

$$\alpha = \frac{4\pi f k}{c} \tag{15}$$

As the velocity of light in a vacuum, $c = f\lambda$, then the extinction coefficient (k) can be defined as:

$$k = \frac{\alpha\lambda}{4\pi} \tag{16}$$

The variation of extinction coefficient (k) and the absorption coefficient with incident photon wavelength is shown in Fig.7. The measured values of absorption coefficient (α) for all the samples are within the range of 1×10^5 to 4×10^5 cm^{-1} in the visible wavelength region which signifies that the 90 % of the incident photon is absorbed within 1 um of the CdTe films.

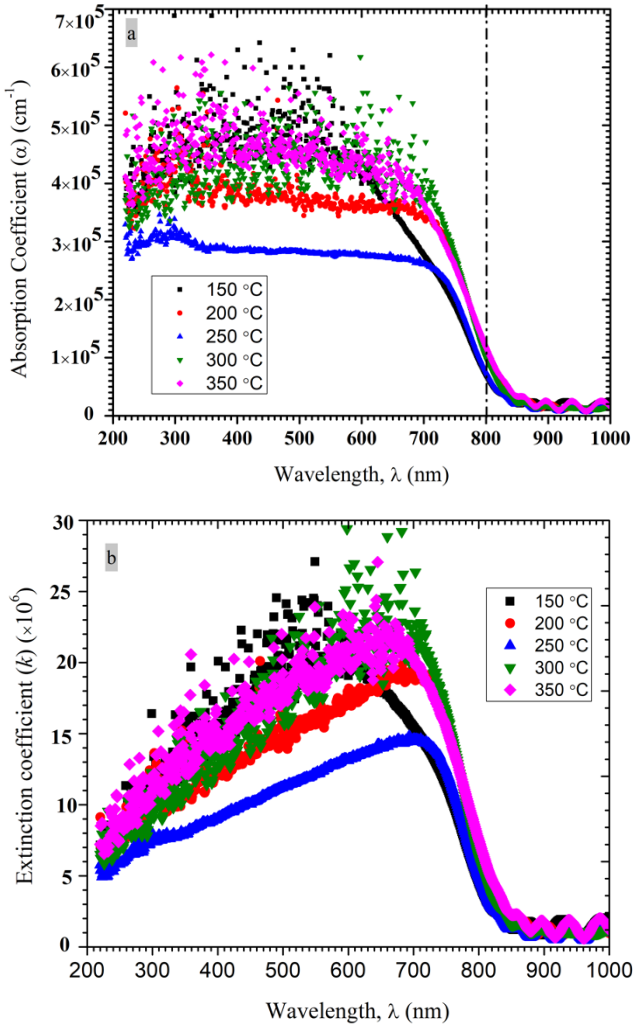

Fig. 7. Wavelength dependent (a) absorption coefficient (α) and (b) extinction coefficient (k) of CdTe thin films grown at different substrate temperatures.

The bandgap Eg of all the deposited film is calculated by using Tauc's relation:

$$\alpha h\nu = B(h\nu - Eg)^m \tag{17}$$

Where B is the energy independent constant, hv is the energy of the incident photon and m is an exponent which signifies the mode of the electronic transition occurs in the solid films and for direct transition, the values of m is considered as 1/2. Then the optical energy gap, Eg of the investigated thin-films, is obtained by extrapolating the linear portion of the graph of $(\alpha h\nu)^2$ versus photon energy ($h\nu$) as shown in Fig. 8 and Fig. 9 respectively. As seen in Fig. 8, the bandgap of the deposited CdS:O/CdS bilayer and CdS:O layer increases from 2.32 eV to 2.56 eV to 2.64 eV respectively relative to CdS films deposited in pure Ar ambient. The improvement of optical bandgap enhances photo current of thin-film solar cells by allowing more photons into the active region. On the other hand, the estimated bandgap of as-deposited CdTe thin films are of 1.50, 1.48, 1.53, 1.54 and 1.51 eV respectively for the substrate temperature 150, 200, 250, 300 and 350 °C as shown in Fig. 9. The estimated value of the optical bandgap is in good agreement with previously reported results as in [29, 32].

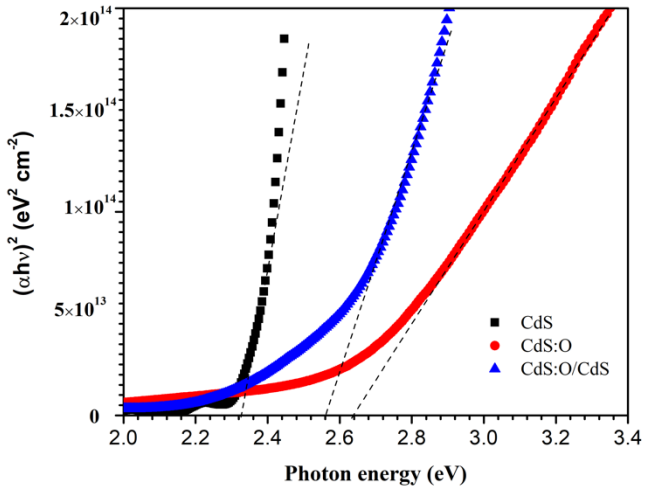

Fig. 8. Tauc plots of as deposited of CdS, CdS:O and CdS:O /CdS layer.

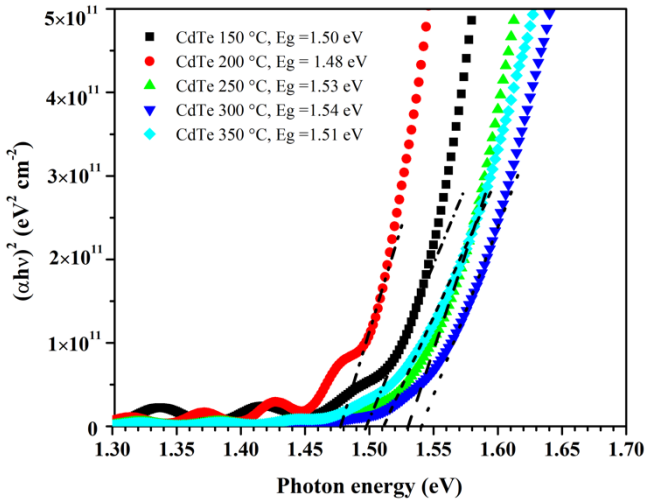

Fig. 9. Tauc plots of as deposited CdTe thin-films for different substrate temperature

3.3. Surface morphology analysis

The surface morphology of the CdTe film deposited at 250 °C was inspected by field emission scanning electron

microscopy (SEM). The SEM image displays homogenous, very compact, pinhole free and a clear faceted morphology of the as-deposited CdTe thin films as shown in Fig. 10. The average grain size of the deposited films is around 127 nm which was calculated using Image J software. Fig. 11 displays the prominent peaks of 'Cd' and 'Te' at 3.2 keV and 3.8 keV respectively in EDX spectrum and the surface compositional study shows Te-rich stoichiometry of the deposited films.

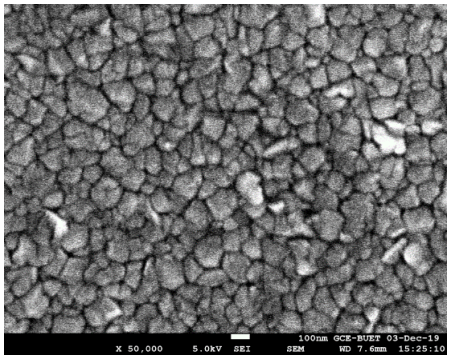

Fig. 10. SEM image of CdTe thin films deposited at 250 °C.

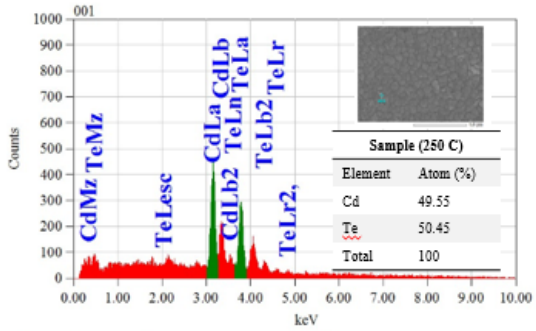

Fig. 11. EDX analysis and mapping of the CdTe thin films deposited at 250 °C.

3.4. Raman spectroscopy

All the deposited CdTe films were analysed with Raman scattering with the high-resolution micro-Raman spectrometer, Horiba Jobin Yvon HR800, at room temperature and atmospheric pressure to investigate the quality and phases of CdTe synthesized films. The Raman spectra are shown in Fig.12, and this spectrum are recorded by using the excitation wavelength of 785 nm from a class 3 B laser source for the planar substrate in the frequency range of 100–1000 cm^{-1}. The measured peaks were fitted with a Lorentzian profile to investigate the impurities in the deposited films. Raman spectra of all the investigated films exhibit a prominent peak at 163.5 cm-1 which is associated with CdTe longitudinal optical (LO) phonon. In Fig.9, there is no existence of A1 mode, double degenerate mode E and the transversal optic (TO) phonon of the CdTe which were located at 121, 139 and 141 cm^{-1}, respectively in comparison with other related works [23, 44-46]. Additionally, the first, second, third and fourth harmonic of LO phonon of CdTe were observed at 328.7, 490.5, 654 and 817.5 cm^{-1} which signifies only the presence of CdTe phases over the entire region of the substrate.

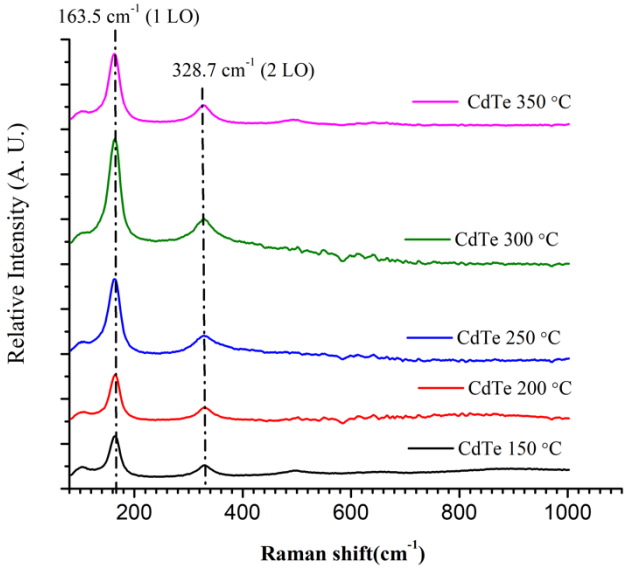

Fig. 12. Raman spectra of RF sputtered CdTe thin films for different substrate temperature.

4. Conclusion

In summary, we report the effects of substrate temperature on the structural and optical properties of RF sputtered CdTe thin films as an absorber material for thin-film solar cell applications. The result reveal that the substrate temperature plays a vital role in the nucleation of CdTe thin films on CdS:O/CdS stack in pure Ar ambient. The CdS:O/CdS bilayer improves the spectral response towards the short wavelength region of the photon flux and net increases of optical bandgap 10.32 % in comparison with the pure CdS layer. The thickness of the deposited films is found to be increasing as the substrate temperature increases from 150°C and reaches the maximum (2.82 um) at 250 °C. The XRD spectra reveal the best crystallinity and greater crystallite size of the deposited films at the substrate temperature 250 and 300 °C respectively. The SEM micrograph displays pinhole-free, smooth and compact CdTe thin films grew over CdS:O/CdS bilayer and the Raman study confirms only the presence of LO mode of CdTe over the entire region of study for all the deposited CdTe films. The CdTe films absorbed the incident photon below 800 nm of wavelength completely and show good optical transmission beyond 820 nm wavelength. In addition tailoring of optical bandgap (1.48 eV to 1.54 eV) was observed as the substrate temperature increase from 150 to 350 °C. Hence, considering the optical and structural properties of the as-deposited CdTe films, the optimum substrate temperature for growing CdTe film on the glass substrate is residing between 250 to 300 °C. Therefore, these results may be useful either for CdTe solar cell fabrications or for other optoelectronic device applications.

Acknowledgement

We would like to express our sincere gratitude to the Department of Electrical and Electronic Engineering, Chittagong University of Engineering and Technology (CUET), Chittagong-4349 for providing the research grant

through HEQEP (CP- 3200). We also express sincere thank to Industrial Physics Division, BCSIR, Dhaka, Department of Glass and Ceramic Engineering, Bangladesh University of Engineering and Technology (BUET) and Materials Science Division, Atomic Energy Centre, Bangladesh Atomic Energy Commission, Dhaka for their valuable suggestions and assistance in characterizing the deposited samples.

References

[1] W. K. Metzger, S. Grover, D. Lu, E. Colegrove, J. Moseley, C. L. Perkins, X. Li, R. Mallick, W. Zhang, R. Malik, J. Kephart, C.-S. Jiang, D. Kuciauskas, D. S. Albin, M. M. Al-Jassim, G. Xiong and M. Gloeckler, "Exceeding 20% efficiency with in situ group V doping in polycrystalline CdTe solar cells," Nat. Energy, vol. 4, no. 10, pp. 837–845, 2019. (Article)

[2] Z. Fang, X. C. Wang, H. C. Wu, and C. Z. Zhao, "Achievements and challenges of CdS/CdTe solar cells," Int. J. Photoenergy, vol. 2011, no. 1, 2011. (Article)

[3] Martin A. Green, Yoshihiro Hishikawa, Ewan D. Dunlop, Dean H. Levi, Jochen Hohl-Ebinger, Masahiro Yoshita, and Anita W.Y. Ho-Baillie, "Solar cell efficiency tables (Version 53)," vol. 2, no. November 2018, pp. 3–12, 2019. (Article)

[4] A. Kowsar, M. Rahaman, M. S. Islam, A. Y. Imam, S. C. Debnath, M. Sultana, M. A. Hoque, A. Sharmin, Z. H. Mahmood, S.F. U. Farhad, "Progress in major thin-film solar cells: Growth technologies, layer materials and efficiencies," International Journal of Renewable Energy Research (IJRER), vol. 9, no. 2, pp. 579–597, 2019. (Article)

[5] K. Lynn, T. Ablekim, and S. Swain, "Solar cells based on cadmium telluride with an open-circuit voltage greater than 1V," SPIE Newsroom, pp. 1–2, 2016. (letter)

[6] Marc Burgelman, Cadmium Telluride Thin Film Solar Cells: Characterization, Fabrication and Modeling, John Wiley & Sons Ltd, 2006, ch. 7. (Book Chapter)

[7] A. McEvoy, T. Markvart and L. Castaner, Handbook of Photovoltaics: Fundamentals and Applications, 2 ed. Academic Press, pp. 1204, 2012. (Book)

[8] S. Kasap and P. Capper, Springer Handbook of Electronic and Photonic Materials, 2 ed., Springer International Publishing, 2017, ch. 16. (Book Chapter)

[9] A. Luque and S. Hegedus, Handbook of Photovoltaic Science and Engineering. John Wiley & Sons Ltd., 2011, ch. 14. (Book Chapter)

[10] S. G. Kumar and K. S. R. K. Rao, "Physics and chemistry of CdTe/CdS thin film heterojunction photovoltaic devices: Fundamental and critical aspects," Energy Environ. Sci., vol. 7, no. 1, pp. 45–102, 2014. (Article)

[11] J. Sites and J. Pan, "Strategies to increase CdTe solar-cell voltage," Thin Solid Films, vol. 515, no. 15 SPEC. ISS., pp. 6099–6102, 2007. (Article)

[12] R. M. Geisthardt, M. Topič, and J. R. Sites, "Status and Potential of CdTe Solar-Cell Efficiency," IEEE J. Photovoltaics, vol. 5, no. 4, pp. 1217–1221, 2015. (Article)

[13] T. Ablekim, S. K. Swain, W. J. Yin, K. Zaunbrecher, J. Burst, T. M. Barnes, D. Kuciauskas, Su-Huai Wei and K. G. Lynn, "Self-compensation in arsenic doping of CdTe," Sci. Rep., vol. 7, no. 1, pp. 1–9, 2017. (Article)

[14] J. M. Burst, J. N. Duenow, D. S. Albin, E. Colegrove, M. O. Reese, J. A. Aguiar, C.-S. Jiang, M. K. Patel, M. M. Al-Jassim, D. Kuciauskas, S. Swain, T. Ablekim, K. G. Lynn and W. K. Metzger,"CdTe solar cells with open-circuit voltage breaking the 1V barrier," Nat. Energy, vol. 1, no. 4, 2016. (Article)

[15] J. N. Duenow, J. M. Burst, D. S. Albin, M. O. Reese, S. A. Jensen, S. W. Johnston, D. Kuciauskas, S. K. Swain, T. Ablekim, K. G. Lynn, A. L. Fahrenbruch, and W. K. Metzger, "Relationship of Open-Circuit Voltage to CdTe Hole Concentration and Lifetime," IEEE J. Photovoltaics, vol. 6, no. 6, pp. 1641–1644, 2016. (Article)

[16] S. Deivanayaki, P. Jayamurugan, R. Mariappan, V. Ponnuswamy, "Optical and structural characterization of CdTe thin films by chemical bath deposition technique," Chalcogenide Lett. 2010, 7, 159–163. (Article)

[17] N. K. Das, S. A. Razi, K. S. Rahman, M. A. Matin, and N. Amin, "Electrical Properties of CSS Deposited CdTe Thin Films for Solar Cell Applications," 1st International Conference on Advances in Science, Engineering and Robotics Technology (ICASERT-2019), 2019. (Conference Paper)

[18] N.A. Khan, K.S. Rahman, K.A. Aris, A.M. Ali, Halina Misran, M. Akhtaruzzaman, S.K. Tiong and N. Amin, "Effect of laser annealing on thermally evaporated CdTe thin films for photovoltaic absorber application," Sol. Energy, vol. 173, no. June, pp. 1051–1057, 2018. (Article)

[19] Maitry Dey, N. K. Das, M. A. Matin, "Effect of Thermally Evaporated n-CdTe Thin Film on Homojunction CdTe Solar Cell," 5th International Conference on Advances in Electrical Engineering (ICAEE-2019), 2019. (Conference Paper)

[20] A. Gupta and A. D. Compaan, "All-sputtered 14% CdS/CdTe thin-film solar cell with ZnO: Al transparent conducting oxide," Appl. Phys. Lett., vol. 85, no. 4, pp. 684–686, 2004. (Article)

[21] S. D. Gunjal, Y. B. Khollam, S.R. Jadkar, T. Shripathi, V.G. Sathe, P.N. Shelke, M.G. Takwale, K.C. Mohite,"Spray pyrolysis deposition of p-CdTe films: Structural, optical and electrical properties," Sol. Energy, vol. 106, pp. 56–62, 2014. (Article)

[22] T. Wang, S. Du, W. Li, C. Liu, J. Zhang, L.Wu, B. Li and G. Zeng, "Control of Cu doping and CdTe/Te

interface modification for CdTe solar cells," Mater. Sci. Semicond. Process., vol. 72, no. September, pp. 46–51, 2017. (Article)

[23] S. Azmi, M. Nohair, M. El Marrakchi, E. Khoumri, and M. Dabala, "Effect of the Complexing Agents on the Properties of Electrodeposited CZTS Thin Films," *7th International Conference on Renewable Energy Research and Applications (ICRERA)*, pp. 1346-1351, 2018. (Conference Paper)

[24] I. M. Dharmadasa, O. K. Echendu, F. Fauzi, N. A. Abdul-Manaf, O. I. Olusola, H. I. Salim, M. L. Madugu and A. A. Ojo, "Improvement of composition of CdTe thin films during heat treatment in the presence of CdCl 2," J. Mater. Sci. Mater. Electron., vol. 28, no. 3, pp. 2343–2352, 2017. (Article)

[25] D. A. Lamb, S. J. C. Irvine, A. J. Clayton, G. Kartopu, V. Barrioz, S. D. Hodgson, M. A. Baker, R. Grilli, J. Hall, C. I. Underwood, and R. Kimber, "Characterization of MOCVD Thin-Film CdTe Photovoltaics on Space-Qualified Cover Glass," IEEE Journal of Photovoltaics, vol. 6, no. 2, March 2016. (Article)

[26] Y. Gu, H. J. Zheng, X. R. Chen, J. M. Li, T. X. Nie, and X. F. Kou, "Influence of Surface Structures on Quality of CdTe (100) Thin Films Grown on GaAs(100) Substrates," Chinese Phys. Lett., vol. 35, no. 8, pp. 6–9, 2018. (Article)

[27] A. D. Compaan and J. R. Sites and R. W. Birkmire and C. S. Ferekides and A. L. Fahrenbruch, "Critical Issues and Research Needs for CdTe-Based Solar Cells," Electrochemical Society Symposium Proceedings, pp. 241—251, 1999. (Conference Paper)

[28] Martín-Tovar, E.A.; Castro-Rodríguez, R.; Iribarren, A. Isoelectronic CdTe-doped ZnO thin films grown by PLD. Mater. Lett. Vol. 139, pp. 352–354, 2015. (letter)

[29] P.M. Kaminski, A. Abbas, C. Chen, S. Yilmaz, F. Bittau, J.W. Bowers and J.M. Walls, "Internal strain analysis of CdTe thin films deposited by pulsed DC magnetron sputtering," 2015 IEEE 42nd Photovolt. Spec. Conf. PVSC 2015, 2015. (Conference Paper)

[30] R. Kulkarni, A. Pawbake, R. Waykar, A. Jadhavar, A. Rokade, S. Rondiya, S. Karpe, K. Diwate, A. Funde. V. Sharma, G. Lonkar and S. Jadkar,"Substrate temperature dependent structural, optical, morphology and electrical properties of RF sputtered CdTe thin films for solar cell application," J. Mater. Sci. Mater. Electron., vol. 27, no. 12, pp. 12405–12411, 2016. (Article)

[31] R. R. Kulkarni, A. S. Pawbake, R. G. Waykar, S. R. Rondiya, A. A. Jadhavar, S. M. Pandharkar, S. D. Karpe, K.D. Diwate, and S. R. Jadkar, "Properties of RF sputtered cadmium telluride (CdTe) thin films: Influence of deposition pressure," AIP Conf. Proc., vol. 1724, 2016. (Conference Paper)

[32] Z. Ghorannevis, E. Akbarnejad, and M. Ghoranneviss, "Effects of various deposition times and RF powers on CdTe thin film growth using magnetron sputtering," J. Theor. Appl. Phys., vol. 10, no. 3, pp. 225–231, 2016. (Article)

[33] N. E. Gorji, "Electrical and optical characterization of R.F.-sputtered CdTe thin films," IEEE Trans. Device Mater. Reliab., vol. 14, no. 4, pp. 983–988, 2014. (Article)

[34] X. Wu, "High-efficiency polycrystalline CdTe thin-film solar cells," Sol. Energy, vol. 77, no. 6, pp. 803–814, 2004. (Article)

[35] N. R. Paudel, J. D. Poplawsky, K. L. Moore, and Y. Yan, "Current Enhancement of CdTe-Based Solar Cells," IEEE J. Photovoltaics, vol. 5, no. 5, pp. 1492–1496, 2015. (Article)

[36] N. K. Das, J. Chakrabartty, S. F. U. Farhad, M. A. Matin, and N. Amin, "Effect of growth temperature on the structural and optical properties of CdS:O thin films for CdTe solar cells," 4th EICT-2019, December 2019, Bangladesh. (Conference Paper)

[37] N. K. Das, S. A. Razi, K. S. Rahman, M. A. Matin, and N. Amin, "Electrical Properties of CSS Deposited CdTe Thin Films for Solar Cell Applications," in 1st ICASERT-2019, September 2019, Bangladesh. (Cnference Paper)

[38] M. A. Islam, M. S. Hossain, M. M. Aliyu, P. Chelvanathan, and Q. Huda, "Comparison of Structural and Optical Properties of CdS Thin Films Grown by CSVT , CBD and Sputtering Techniques," Energy Procedia, vol. 33, pp. 203–213, 2013. (Conference Paper)

[39] J C Manifacier, J Gasiot and J P Fillard, " A simple method for the determination of the optical constants n, k and the thickness of aweakly absorbing thin film," J. Phys. E: Sci. Instrum, 1976. (Article)

[40] S. Chander and M. S. Dhaka, "Thermal evolution of physical properties of vacuum evaporated polycrystalline CdTe thin films for solar cells," J. Mater. Sci. Mater. Electron., vol. 27, no. 11, pp. 11961–11973, 2016. (Article)

[41] K. S. Rahman, M. N. Harif, H. N. Rosly, M. I. B. Kamaruzzaman, M. Akhtaruzzaman, M. Alghoul, H. Misran and N. Amin, "Influence of deposition time in CdTe thin film properties grown by Close-Spaced Sublimation (CSS) for photovoltaic application," Results Phys., vol. 14, no. May, p. 102371, 2019. (Article)

[42] D. Bonnet and P. Meyers, "Cadmium-telluride - Material for thin film solar cells," J. Mater. Res., vol. 13, no. 10, pp. 2740–2753, 1998.

[43] N. R. Paudel, K. A. Wieland, and A. D. Compaan, "Ultrathin CdS/CdTe solar cells by sputtering," Sol. Energy Mater. Sol. Cells, vol. 105, pp. 109–112, 2012. (Article)

[44] G. Morell, A. R. Figueroa, R. S. Katiyar, M. H. Farias, F. J. E. Beltran, O. Z. Angel and F. S. Sinencio, "Raman spectroscopy of oxygenated amorphous CdTe

films," J. Raman Spectrosc., vol. 25, no. 3, pp. 203–207, 1994. (Article)

[45] F. M. Flores, J.G. Q. Galván, A. G. Cervantes, J.S. A. Cerón, A. H. Hernández, J. S. Salazar, J. S. Cruz, S.A. M. Hernández, M. de la L. Olvera, J.G. M. Álvarez, M. M. Lira, G. C. Puente, "CdTe thin films grown by pulsed laser deposition using powder as target: Effect of substrate temperature," J. Cryst. Growth, vol. 386, no. May 2018, pp. 27–31, 2014. (Article)

[46] J. Rangel-Cárdenas and H. Sobral, "Optical absorption enhancement in CdTe thin films by microstructuration of the silicon substrate," Materials (Basel)., vol. 10, no. 6, 2017. (Article)